Chemical Research in Toxicology

Article

pubs.acs.org/crt

Multiwalled Carbon Nanotubes Induce a Fibrogenic Response by Stimulating Reactive Oxygen Species Production, Activating NF-κB Signaling, and Promoting Fibroblast-to-Myofibroblast Transformation

Xiaoqing He,[†] Shih-Houng Young,[‡] Diane Schwegler-Berry,[‡] William P. Chisholm,[§] Joseph E. Fernback,[∥] and Qiang Ma*[,†]

[†]Receptor Biology Laboratory, Toxicology and Molecular Biology Branch, [‡]Pathology and Physiology Research Branch, and [§]Exposure Assessment Branch, Health Effects Laboratory Division, National Institute for Occupational Safety and Health, Centers for Disease Control and Prevention, Morgantown, West Virginia 26505, United States

[∥]Chemical Exposure & Monitoring Branch, Division of Applied Research and Technology, National Institute for Occupational Safety and Health, Centers for Disease Control and Prevention, Cincinnati, Ohio 45226, United States

ABSTRACT: Carbon nanotubes (CNTs) are novel materials with unique electronic and mechanical properties. The extremely small size, fiberlike shape, large surface area, and unique surface chemistry render their distinctive chemical and physical characteristics and raise potential hazards to humans. Several reports have shown that pulmonary exposure to CNTs caused inflammation and lung fibrosis in rodents. The molecular mechanisms that govern CNT lung toxicity remain largely unaddressed. Here, we report that multiwalled carbon nanotubes (MWCNTs) have potent, dose-dependent toxicity on cultured human lung cells (BEAS-2B, A549, and WI38-VA13). Mechanistic analyses were carried out at subtoxic doses (≤20 μg/mL, ≤ 24 h). MWCNTs induced substantial ROS production and mitochondrial damage, implicating oxidative stress in cellular damage by MWCNT. MWCNTs activated the NF-κB signaling pathway in macrophages (RAW264.7) to increase the secretion of a panel of cytokines and chemokines (TNFα, IL-1β, IL-6, IL-10, and MCP1) that promote inflammation. Activation of NF-κB involved rapid degradation of IκBα, nuclear accumulation of NF-κBp65, binding of NF-κB to specific DNA-binding sequences, and transactivation of target gene promoters. Finally, MWCNTs induced the production of profibrogenic growth factors TGFβ1 and PDGF from macrophages that function as paracrine signals to promote the transformation of lung fibroblasts (WI38-VA13) into myofibroblasts, a key step in the development of fibrosis. Our results revealed that MWCNTs elicit multiple and intertwining signaling events involving oxidative damage, inflammatory cytokine production, and myofibroblast transformation, which potentially underlie the toxicity and fibrosis in human lungs by MWCNTs.

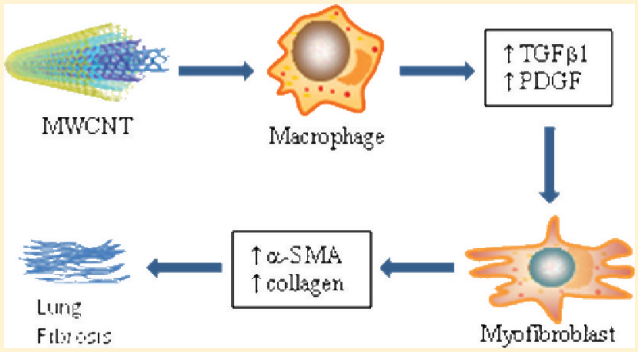

INTRODUCTION

Pulmonary fibrosis can arise from exposure to a variety of environmental and occupational agents including fibers, particles, metals, pesticides, anticancer drugs, and microbes.[1−5] The underlying mechanism(s) for lung fibrosis remains largely unclear. On the other hand, several cellular responses are commonly observed in agent-induced lung fibrosis, including injury to bronchial and alveolar epithelium, activation of macrophages for stimulation of inflammation, and proliferation and transformation of fibroblasts into myofibroblasts for synthesis, deposition, and remodeling of matrix.[6−8] At a molecular level, these fibrogenic responses are believed to be mediated through specific signaling pathways that are key to the development of lung fibrosis but are poorly understood at the present time. Conceivably, elucidating the molecular determinants and pathways that govern lung fibrosis by fibrogenic agents has a number of applications for human health including: risk assessment through the development of biomarkers and high throughput screening; early diagnosis of lung toxicity and fibrosis by detecting molecular changes that occur prior to permanent, structural pathology; drug targeting of critical pathways and molecules; and finally, product improvement by identifying and eliminating structures and properties that cause toxicity and fibrosis.

Carbon nanotubes (CNTs) are recently developed, promising nanomaterials with remarkable electroconducting property, physical strength, and surface chemistry.[9] Structurally, CNTs are molecular-scale tubes of graphitic carbon, either single-walled (SWCNT) or multiwalled (MWCNT). The tremendous

Received: August 16, 2011
Published: November 14, 2011

dx.doi.org/10.1021/tx200351d | Chem. Res. Toxicol. 2011, 24, 2237−2248

increase in the production of CNT in recent years raised concerns over the human health risk of engineered nanotubes: Their extremely small size (nano meters in diameter) makes them airborne and easily inhaled into the human lungs; the high length-to-diameter ratio (up to 10^8-fold) and large surface area may lead to toxic effects similar to those of silica and asbestos (i.e., lung fibrosis and mesothelioma).[10−15] Therefore, assessing the potential toxicity of CNT in humans is a pressing issue, even though no pathological conditions have been identified in humans from CNT exposure so far.[12,16,17]

Data on the adverse health effects of CNT to date are limited, and some appear controversial, partly due to the fact that many parameters of CNT, such as structure, size distribution, surface area, surface charge and chemistry, agglomeration state, and purity, influence their reactivity with the human body; moreover, these parameters can vary from sample to sample considerably. Nevertheless, current data indicated that many CNTs can enter human cells to accumulate in the cytoplasm and cause cell death,[18] penetrate tissue structures to migrate and cause lesions in remote areas,[13,14,19] and induce inflammation, epithelioid granulomas, and interstitial or pleural fibrosis in the lungs of rodents.[17,20−24] The cellular and molecular mechanisms by which CNTs damage cells and cause inflammation and fibrosis in the lungs remain largely unaddressed. Given the extreme paucity of human data and very limited animal models for CNT health effects, elucidating the interactions between the CNTs and the host at cellular and molecular levels is not only attainable but also necessary for accurate risk assessment, intervention of toxicity, and CNT product improvement.

The NF-κB proteins form homo- or heterodimers to mediate diverse functions, such as inflammation, immune response, apoptosis, and cell proliferation.[25] Unactivated NF-κB is tightly repressed by a group of inhibitory proteins (IκBs) in the cytoplasm. During lung fibrosis, NF-κB is activated to control the production of inflammatory cytokines and chemokines from both macrophages and lung epithelial cells. Activation may involve the canonical pathway that converges on a multisubunit IκB kinase complex (IKK) leading to the ubiquitination and degradation of phosphorylated IκB through the SCF E3-dependent ubiquitination and proteasomal degardation. Alternatively, a noncanonical pathway can be activated to phophorylate RelB-bound p100, causing protease cleavage of the protein and formation of an active p52/RelB complex for gene transcription. Whether CNTs activate the NF-κB pathways to influence their toxicity is unclear.

Transforming growth factor β1 (TGFβ1) and platelet-derived growth factor (PDGF) are two potent regulators of extracellular matrix formation and remodeling critical for the development of fibrosis.[6,7,26,27] TGFβ1 was associated with progressive lung fibrosis in humans and was elevated in the lungs of patients with idiopathic pulmonary fibrosis and in animal models of lung fibrosis.[28] TGFβ1 stimulates the differentiation of lung fibroblasts into myofibroblasts, which synthesize collagen 1 and α-smooth muscle actin (αSMA) for matrix deposition and remodeling during fibrosis. PDGF acts as a potent mitogen and chemoattractant for fibroblasts and myofibroblasts, thereby promoting fibrosis.[6] PDGF has been implicated in the development of asbestosis and coal workers' pneumoconiosis from the inhalation of asbestos fiber and coal dust particle. NF-κB may regulate TGFβ and PDGF functions in fibrosis by influencing the TGFβ signaling pathway for collagen synthesis[29] and the transcription of PDGF.[30,31] The roles of TGFβ1, PDGF, and myofibroblast transformation in CNT-induced fibrotic reactions in the lungs have not been investigated.

In light of the high potential of CNT to cause toxicity and fibrotic lesions in human lungs and the lack of understanding of the mechanism for lung fibrosis by CNT, we carried out this study to characterize MWCNT toxicity and identify the molecular events that govern the inflammatory and fibrogenic responses to MWCNT in human lung cells. Our data revealed that (1) MWCNT caused dose-dependent toxicity in human bronchial and alveolar epithelial cells and interstitial fibroblasts by causing mitochondrial damage and oxidative stress, (2) MWCNT induced a panel of cytokines and chemokines through the activation of NF-κB in macrophages, and (3) MWCNT stimulated the expression and secretion of TGFβ1 and PDGF from lung cells and macrophages to increase the proliferation and transformation of lung fibroblasts into myofibrolasts. Together, these in vitro cellular model-based studies revealed a molecular framework for CNT-induced fibrotic reactions in the lungs that potentially fills the knowledge gap in the understanding of molecular mechanisms for CNT-induced lung toxicity.

MATERIALS AND METHODS

Materials. MWCNTs were purchased from Sigma-Aldrich (St. Louis, MO). According to the supplier, MWCNTs were >99% pure on a carbon basis by X-ray diffraction and 99% pure on a nanotube basis by high-resolution transmission electron microscopy (HRTEM). A patented process involving decomposition of carbon monoxide over a Co−MgO catalyst at about 600 °C was used to produce the MWCNT. The nanotubes were then treated with diluted hydrochloric acid to completely remove the catalyst. No metals were detected by X-ray diffraction. Cell lines, antibodies, and other reagents were described below.

Dispersion of MWCNTs. Two milligrams of MWCNTs was dispersed in 1 mL of a cell culture medium containing 1% fetal bovine serum (FBS) through vortex (three times, 2 min each) and sonication (three times, 30 s each; 40% output; Ultrasonic Processor, GE 70T, Fisher Scientific, Pittsburgh, PA) in a biological safety hood. Dispersed MWCNTs were stored as a stock solution and were further diluted with the culture medium and resonicated within 20 min before use.

Transmission Electron Microscopy (TEM) and HRTEM. The dispersed MWCNT stock solution prepared above was diluted at 1:1000 into double-distilled H_2O and loaded within 30 min of preparation for imaging. A drop of ∼0.1 mL was deposited onto a Formvar-coated copper grid and allowed to air dry. Images were photographed on a JEOL 1220 TEM. For HRTEM, MWCNTs were dispersed into ethanol with sonication. The samples were deposited on a 200 mesh copper TEM grid with a lacy carbon film. The grid was examined using the JEOL 2100F STEM at an accelerating voltage of 200 keV. Images were obtained at various magnifications in a bright field TEM mode.

Fourier Transform Infrared Spectroscopy (FTIR). FTIR was carried out to detect potential functionalization of MWCNTs with carboxyl groups from acid wash during manufacture. A few drops of acetone and methanol suspension containing approximately 100 μg of MWCNTs was air-dried on a 2 mm × 13 mm KBr disk (Spectra-Tech Inc. Part No. 7000-302, Oak Ridge, TN). A second KBr disk was placed over the first, and the pair was mounted in a sample holder with 10 mm aperture. The infrared absorbance spectrum of this sample was acquired in direct transmittance mode (32 scans, 4 cm^{-1} resolution) by a Nicolet 6700 FTIR spectrometer (ThermoFisher Scientific, Waltham, MA). Carbonyl groups of carboxylated material display a very strong, narrow feature near 1700 cm^{-1}.[32]

Cell Culture. Human normal bronchial epithelial cell line immortalized with SV40 (BEAS-2B), human normal lung fibroblast cell line immortalized with SV40 (WI38-VA13), human lung

carcinoma epithelial cell line (A549), and mouse leukemic monocyte-macrophage cell line (RAW264.7) were purchased from American Type Culture Collection (ATCC, Manassas, VA). BEAS-2B cells were cultured with the bronchial epithelial cell growth medium (BEGM) along with all of the additives from Lonza/Clonetics Corporation (Walkersville, MD). A549 cells were cultured in the Dulbecco's modified Eagle's medium (DMEM) (Invitrogen, Carlsbad, CA) with 10% FBS. WI38-VA13 cells were cultured in the α minimal essential medium (αMEM, Invitrogen) with 10% FBS. RAW264.7 cells were grown in DMEM with 10% FBS.

Because cells were treated with MWCNTs at $\leq$20 μg/mL for most of the experiments, the dispersion medium added to a culture was $\leq$1% of the culture and FBS from the dispersion medium $\leq$0.01%. For cells cultured in media with 10% FBS, the dispersion medium did not change the culture medium composition. For BEAS-2B cells cultured in the BEGM medium, the treatment added 0.01% FBS into the culture. Controls with 1% the dispersion medium without MWCNT were tested to ascertain that no effect from the dispersion medium interfered with BEAS-2B culture and results. No effects of the dispersion medium on BEAS-2B cells were observed in all assays.

Endotoxin Detection. MWCNTs were prepared as a suspension in water at 2 mg/mL. The suspension was mixed by rocking on a platform for 24 h at room temperature. Samples were centrifuged for 10 min, and supernatants were collected and filtered to remove remaining particles. The detection of endotoxin was performed by using the ToxinSensor Chromogenic Limulus Amebocyte Lysate Assay kit according to the manufacturer's instructions (GenScript, Piscataway, NJ).

Cytotoxicity Assay. The CellTiter 96 AQueous One Solution Cell Proliferation Assay kit (Promega, Madison, WI) was used to examine cell proliferation and cytotoxicity. About 1×10^5 cells per well in 100 μL of the culture medium were seeded in 96-well plates for overnight. Cells were treated with MWCNTs by replacing the medium with a fresh medium containing varying concentrations of MWCNTs. Twenty microliters of the CellTiter 96 AQueuos One Solution Reagent was added into each well. The plates were incubated for 3 h at 37 °C in a humidified incubator supplied with 5% CO_2. The absorbance at 490 nm was recorded by using a 96-well plate reader. Parallel wells with no cells but having the medium containing MWCNTs at the same concentration as treated wells were used as the reference control for MWCNTs. The mean absorbance was calculated from three replicates of each exposure and corresponding blank control.

Reporter Assay. RAW264.7 cells stably transfected with the tumor necrosis factor α (TNFα) promoter/Luc reporter or the 5x NF-κB-binding site/Luc reporter were described previously.[33] Cells were treated with MWCNTs for 16 h as indicated. The cells were lysed with the passive reporter lysis buffer (Promega), and cell lysates were vortexed and centrifuged briefly to remove cell debris. Twenty microliters of a supernatant was mixed with 100 μL of the luciferase reagent (Promega). Luciferase activities were detected by using the TD 20/20 luminometer (Agilent Technologies, Santa Clara, CA) and were normalized with protein concentrations.

Immunoblotting. Cells were lysed on ice with a radioimmune precipitation assay (RIPA) buffer containing protease and phosphatase inhibitors for 30 min. The cell lysate was sonicated briefly and centrifuged at 14000*g* for 20 min to remove cell debris. The cell lysate (10–20 μg) was fractionated by 10% sodium dodecyl sulfate–polyacrylamide gel electrophoresis (SDS-PAGE), transferred to polyviinglidene difluoride (PVDF) membranes (Bio-Rad, Hercules, CA), and blocked with 5% nonfat milk in PBST (PBS plus 0.05% Tween-20). The membrane was blotted with a primary antibody at 4 °C overnight with shaking, followed by incubation with a horseradish peroxidase-conjugated secondary antibody for 1 h at room temperature. Protein bands were visualized using enhanced chemiluminescence detection reagents from Amersham Biosciences (Pisctaway, NJ). Actin was blotted as a loading control.

Detection of Cytokines. Macrophages were treated with MWCNTs for 16 h or lipopolysaccharide (LPS) (1 μg/mL) for 5 h. The cell supernatant was collected and stored at −80 °C until use. Cytokines and chemokines were detected by using a mouse cytometric bead array kit and Flex beads (BD biosciences, Franklin Lakes, NJ) and flow cytometry according to manufacturer's instructions.

Reactive Oxygen Species (ROS) Detection. Cells (BEAS-2B, WI38-VA13, and A549) cultured in eight-well chamber slides were treated with MWCNTs for 16 h. Thirty minutes prior to the end of each treatment, dihydroethium (hydroethidine, DHE, Invitrogen) was added at 5 μM as a fluorescent indicator of ROS production. Cells were washed with ice cold phosphate-buffered saline (PBS) for three times to remove free dye. Cells were then fixed in 4% paraformaldehyde and mounted with a mounting solution containing DAPI that counterstains the nucleus. Images were taken with a Zeiss LSM510 confocal microscope using the Rhodamin-DAPI setting and fixed exposure times. The fluorescence intensity was quantified by using the Optimus Version 6.51 software (Media Cybernetics, Silver Springs, MD). Means and standard deviations (SDs) were calculated from five separate fields for each treatment.

Mitochondrial Membrane Potential. Tetramethylrodamine ester (TMRE, Sigma) and Mitotrack deep red 633 (MTDR, Invitrogen) are fluorescent probes that specifically accumulate in the mitochondrial matrix in a mitochondrial-inner-membrane-potential-dependent manner. Cells (BEAS-2B) were cultured in an eight-well chamber slide (for confocal microscopy) or six-well plate (for flow cytometry) and were treated with MWCNTs for 16 h. Forty-five minutes prior to the end of each treatment, 50 nM TMRE and 1 μM MTDR were added to the culture media. Cells were washed three times with ice cold PBS. For confocal microscopy, cells were fixed in 4% paraformaldehyde in the chamber slides and were mounted with a mounting solution containing DAPI to counterstain the nucleus. Images were taken with a Zeiss LSM510 confocal microscope. For flow cytometry, cells were collected to analyze the fluorescence intensity immediately at 585 (FL-2) and 670 nm (FL-3) channels of a FACSCalibur.

Immunofluorescent Staining. Cells (RAW264.7) grown in an eight-well chamber slide were treated with MWCNTs for 16 h. Cells were fixed in 4% paraformaldehyde and permeated in 0.5% Triton X-100. Cells were stained with the anti NF-κBp65 antibody (Santa Cruz Biotechnology, Inc., Santa Cruz, CA) at a 1:1000 dilution in the culture medium containing 1% FBS for 2 h. The cells were washed three times with PBS. An Alexia 488-conjugated secondary antibody was diluted at a 1:500 dilution in the culture medium with 1% FBS and incubated with the cells for 1 h avoiding light. After they were washed with PBS for three times, the cells were mounted with a mounting solution containing DAPI. Images were taken with a Zeiss LSM510 confocal microscope. For detection of fibroblast-to-myofibroblast transformation, Macrophages were treated with MWCNTs for 16 h or LPS for 5 h. The culture medium was collected and centrifuged to remove remaining cells, debris, and MWCNTs. The cell- and MWCNT-free medium was designated as the MWCNT-conditioned medium. WI38-VA13 cells grown in eight-well chamber slides were cultured in the MWCNT-conditioned medium for 24 h. The cells were then fixed, permeated, and stained with an anti-αSMA antibody (Sigma) for overnight, followed by an Alexia-conjugated secondary antibody for 1 h. The nucleus was counterstained with DAPI. Fluorescent images were taken under a Zeiss LSM510 confocal microscope.

Real-Time PCR. BEAS-2B and WI38-VA13 cells were treated with MWCNT at 10 μg/mL for 24 h. LPS at 1 μg/mL for 5 h, and interleukin (IL)-1β (Sino Biological Inc., www.sinobiological.com) at 5 ng/mL for 24 h were used as positive controls. Total RNA was isolated using the Qiagen RNA mini kit (Qiagen, Valencia, CA). Five micrograms of total RNA was reverse transcribed into cDNA using reverse transcriptase III (Invitrogen). TGFβ1 and PDGF cDNAs were then amplified and quantified with gene-specific primers (primer sequences available upon request) by real-time PCR as described previously.[34]

ELISA for NF-κB DNA Binding. Macrophages were treated with MWCNTs at 10 μg/mL for 16 h or LPS at 1 μg/mL for 5 h. Nuclear extracts were prepared by using the Nuclei EZ PREP reagents from Sigma. Ten micrograms of nuclear extracts was added to an ELISA

plate precoated with NF-κB-binding site dsDNA. Bound NF-κB proteins were detected with an anti-NF-κBp65 antibody following the instructions from Cayman (Ann Arbor, MI).

RESULTS

Characterization of MWCNTs. The MWCNTs used in the study have a purity of 99.9% on carbon basis by X-ray diffraction and are 99% of MWCNTs by HRTEM. HRTEM images showed the distinctive crystalline structure of MWCNTs (Figure 1A). The outer diameters of MWCNTs

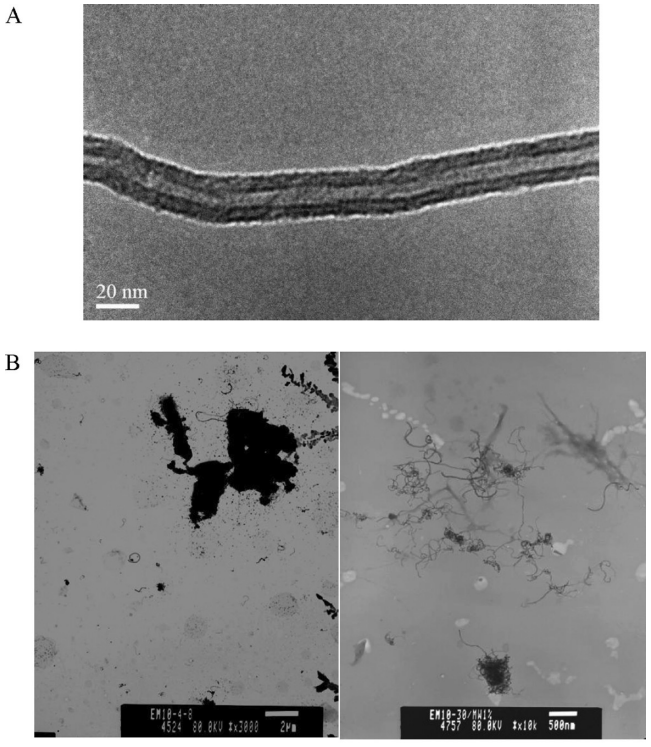

Figure 1. High- and low-resolution transmission electron micrographs of MWCNTs. (A) A representative crystalline structure of MWCNTs from HRTEM showing the distinctive multiwalled nanotube structure. (B) Dispersion of MWCNTs in PBS (left) or the culture medium with 1% FBS (right) from low-resolution TEM showing large agglomerates in PBS and good dispersion in the medium.

range from 6.0 to 13.0 nm (average of 8.7 nm), the inner diameters range from 2.0 to 6.0 nm, and lengths range from 2.5 to 20 μm (average of 10 μm). Trace metal analysis revealed that cobalt is the major metal contaminant with content at ~0.2% and all other metals at or below 10 ppm. Endotoxin contamination of MWCNT was below the level of detection (maximum sensitivity of assay at 0.005 EU/mL). The MWCNT was treated with diluted acid to remove catalyst during manufacture, which potentially introduced carboxyl groups on the surface and ends of the MWCNT. Examination of the MWCNT by FTIR spectroscopy revealed a nearly featureless spectrum typical of pristine CNT, with no infrared lines near 1700 cm^{-1} of carbonyl groups, indicating that there are very few, if any, carbonyl groups on the MWCNT (data not shown).

To disperse MWCNT in solution, 2 mg of MWCNTs was suspended in PBS, a dispersal medium (DM) (Porter et al.),[22] or the culture medium with 1% FBS, respectively. The agglomeration status of MWCNT was analyzed by TEM. Large agglomerates of MWCNTs were found in the PBS suspension, whereas MWCNTs suspended in DM (data not shown) or the culture medium with 1% FBS were well dispersed (Figure 1B). Because the dispersion medium with 1% FBS is compatible with the cell culture conditions, MWCNTs prepared with the dispersion medium were used for all of the following experiments.

Cytotoxicity, ROS Production, and Mitochondrial Damage. Fibrogenic fibers damage the bronchial epithelial, alveolar epithelial, and interstitial (mainly fibroblasts) cells upon entering the lungs, providing the initial stimulus for subsequent inflammation, tissue repair, or fibrosis in the lungs. We first characterized the overall toxicity of MWCNT in human lung cells, including normal bronchial epithelial cells BEAS-2B, normal lung fibroblasts WI38-VA13, and lung alveolar epithelial cells A549. A modified MTT assay was used to measure cell death and proliferation. Parallel controls using the medium containing MWCNTs at the same concentrations as the treatment groups but no cells were used as reference to correct for light absorption from MWCNTs. The three lines of lung cells treated for 1 and 4 days showed dose-dependent but varying degrees of reduction in cell density, revealing increased cell death and/or inhibition of cell proliferation by MWCNTs. BEAS-2B is the most sensitive showing toxicity at 2 μg/mL and nearly total cell death at 200 μg/mL after 4 days of treatment, followed by WI38-VA13 with toxicity beginning at 5 μg/mL and A549 at 20 μg/mL (Figure 2A). After 1 day of treatment, MWCNTs caused significant toxicity at a high dose (200 μg/mL) (data not shown).

Fibrogenic fibers generally do not directly damage DNA and protein but induce the production of ROS to cause oxidative stress in cells. Thus, we examined ROS production as a potential mechanism of cell toxicity by MWCNTs. Fluorescent microscopy using a ROS-sensitive probe, DHE, revealed that, indeed, exposure to MWCNT induced production of ROS in all three cell lines at 20 μg/mL, 16 h (Figure 2B,C). These data indicated that increased production of ROS is a common response to MWCNTs in lung cells at subtoxic doses. For subsequent studies, we chose 20 μg/mL (or less) for 16 h as the treatment to avoid toxicity. This dose range in culture is roughly equivalent to the dose of MWCNT to cause inflammatory response in the lungs on a surface area basis.[13,22] At this dose range, the dispersion medium (corresponding culture medium plus 1% serum) was ≤1% of the culture and FBS from the dispersion medium ≤0.01%, which did not affect cell toxicity, ROS production, and subsequent assays for all cells tested (data not shown).

The mitochondria consume about 90% of the oxygen in the cell for aerobic respiration to produce ATP. They are also responsible for the production of the majority of ROS under normal and pathological conditions. Therefore, we examined mitochondrial damage as a potential mechanism of MWCNT-induced ROS production. TMRE and MTDR are fluorescent probes that specifically accumulate and fluoresce in the mitochondrial matrix in a mitochondrial-inner-membrane-potential-dependent manner. We found that both probes accumulated in the mitochondria in vehicle-treated cells, but accumulation was largely diminished by treatment with MWCNT (20 μg/mL, 16 h), as measured by both confocal fluorescent microscopy and flow cytometry (Figure 3). The results indicated that MWCNT caused substantial loss of the

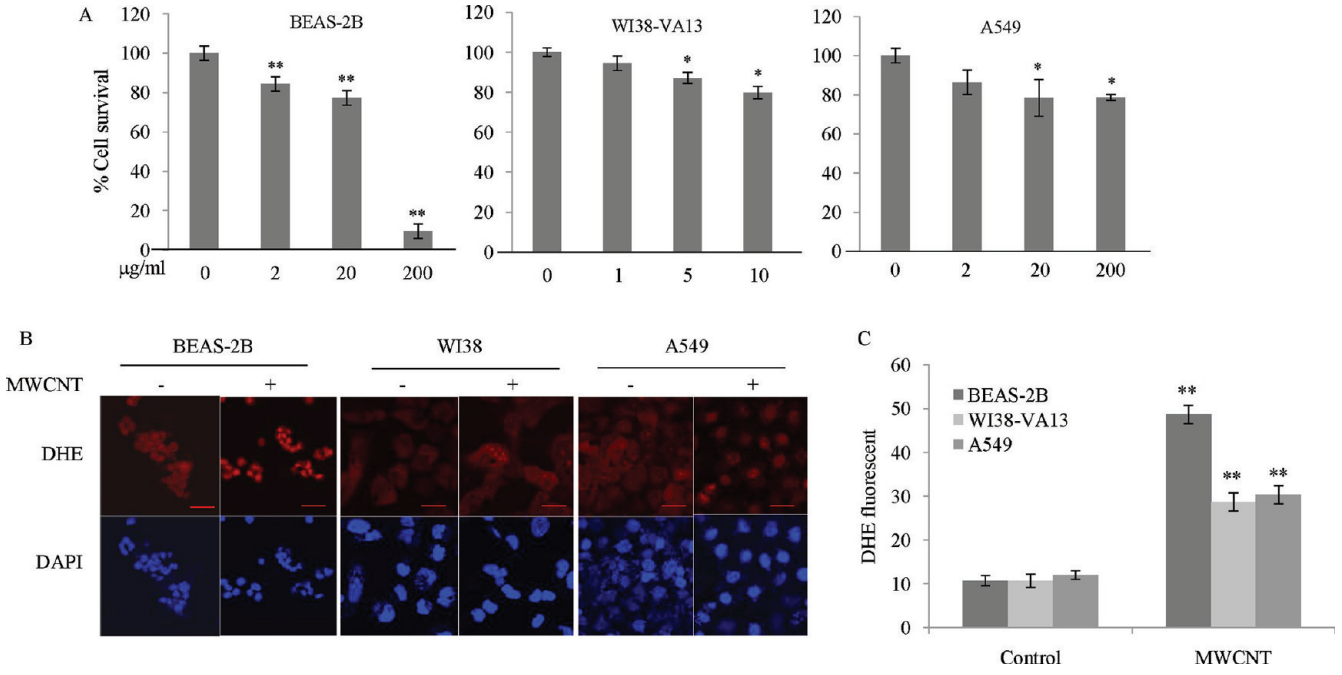

Figure 2. Cytotoxicity and ROS production in human lung cells. (A) Cytotoxicity. BEAS-2B, WI38-VA13 and A549 cells were treated with increasing concentrations of MWCNTs from 0 to 200 μg/mL for 1 and 4 days. Cell proliferation/cell death was assessed using the CellTiter 96 AQueous One Solution Cell Proliferation Assay reagents. Data represent means ± SDs from three samples. *, $p < 0.05$ and **, $P < 0.01$, as compared with the control with no MWCNTs. Shown are toxicities in cells treated for 4 days. Toxicity at 1 day after treatment was significant only at the dose of 200 μg/mL (data not shown). (B) ROS production. BEAS-2B cells were treated with MWCNT at 20 μg/mL for 16 h. ROS production was measured with confocal fluorescence miroscopy using fluorescence probe DHE added to the cells 30 min prior to the end of each treatment. The nucleus was stained with DAPI to show the cell population. (C) Quantification of panel B from five separate fields.

electric potential across the inner membrane of the mitochondria, resulting in diffusion of the probes in the cells. Together, the findings suggest that MWCNT damage the mitochondria to increase ROS production and, thereby, cause toxicity in lung cells.

Induction of Cytokines and Chemokines through NF-κB Signaling. The production of inflammatory cytokines and chemokines from macrophages and lung epithelial cells is a hallmark of the pulmonary response to fibrogenic fibers. We analyzed MWCNT-stimulated production of a panel of representative cytokines and chemokines, whose expressions are commonly altered during inflammation. TNFα is a multifunctional cytokine involved in systemic inflammation and is highly inducible by various inflammatory stimuli. We first tested if MWCNT induces the expression of a luciferase reporter gene stably integrated into the genome of RAW264.7, a widely used macrophage cell line, under the control of the mouse TNFα gene promoter. LPS, a potent inducer of TNFα expression, was used as a positive control. Figure 5A showed that both LPS (1 μg/mL, 5 h) and MWCNT (20 μg/mL, 16 h) strongly increased the luciferase reporter activity, indicating reporter gene induction. We then examined whether MWCNT induces endogenous cytokines and chemokines. RAW264.7 macrophages were treated with MWCNT or LPS. TNFα was increased in the culture medium of MWCNT-treated cells dose dependently (Figure 4B). IL-1β, a pro-inflammatory cytokine induced by microbial infection, was significantly increased at 20 μg/mL (Figure 4C). IL-6, a pro-inflammatory cytokine that stimulates the immune response to damaged tissues, was significantly increased at 2 and 20 μg/mL (Figure 4D). IL-10, an anti-inflammatory cytokine that blocks NF-κB signaling and inhibits the production of pro-inflammatory cytokines, was induced strongly by LPS and MWCNT (Figure 4E). Monocyte chemotactic protein-1 (MCP1), a monocyte chemoattractant of the CC chemokine family, was induced by MWCNT at both 2 and 20 μg/mL; induction at 20 μg/mL was even higher than that by LPS (Figure 4F). IFN-γ, a cytokine critical for innate and adaptive immunity against virus, intracellular bacteria, and tumor cells, was not significantly affected by LPS or MWCNT (Figure 4G). IL-12, an IL produced in the body upon antigenic stimulation, was expressed at low levels (less than 4 pg/mL) and was not significantly changed by LPS or MWCNT treatment (data not shown). Therefore, MWCNTs directly induce inflammatory cytokines and chemokines including TNFα, IL-1β, IL-6, IL-10, and MCP1 to mediate inflammatory response.

NF-κB controls the basal and inducible expression of inflammatory mediators. Induction of the luciferase reporter under the control of TNFα promoter that contains multiple NF-κB-binding sites by MWCNT implicates NF-κB in the induction of cytokine expression by MWCNTs. To address the possibility, we examined whether MWCNTs activate the NF-κB pathway as a molecular mechanism for induction of inflammatory cytokines and chemokines. RAW264.7 macrophages stably transfected with a synthetic, five copy NF-κB-binding site/Luc reporter expression construct were treated with MWCNTs and LPS (positive control for induction). Strong luciferase activities were detected in LPS or MWCNT-treated cells (Figure 5A). The results indicated that MWCNTs could activate the NF-κB target gene promoter to induce gene transcription.

NF-κB can be activated via the conanical or nonconanical pathway. We found that MWCNT induced a sharp reduction in the level of IκBα protein within 30 min of treatment similarly to

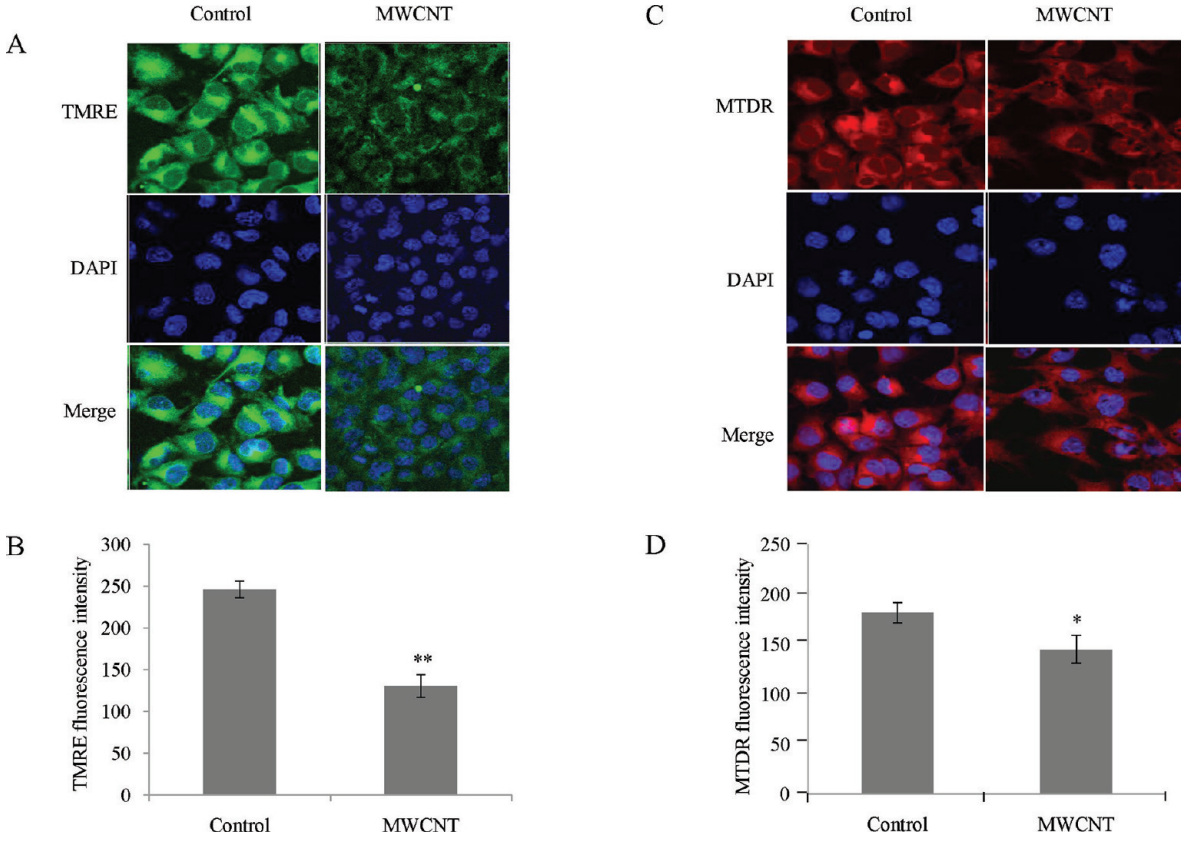

Figure 3. Effect on mitochondrial inner membrane potential. BEAS-2B cells were treated with MWCNTs at 20 μg/mL for 16 h. Damage to mitochondria was assessed using fluorescent probes TMRE (A and B) and MTDR (C and D), both of which accumulate in the mitochondrial matrix in a mitochondrial-inner-membrane-potential-dependent manner. Representative micrographs were taken with confocal microscopy (A and C). Quantification of fluorescence was performed with flow cytometry (B and D), and results represent TMRE or MTDR fluorescence intensity. Data are means ± SDs from three samples. *, $p < 0.05$, and **, $p < 0.01$, as compared with control.

LPS (Figure 5B). Both LPS and MWCNTs induced strong nuclear localization of NF-κB as revealed by immunoblotting of NF-κB in nuclear fractions or by confocal fluorescent microscopy of cells treated with LPS or MWCNTs (Figure 5C,D). Finally, NF-κB binding to the NF-κB-binding sequences was examined, in which nuclear extracts from macrophages treated with MWCNTs or LPS was assayed for binding to NF-κB binding sequences in an ELISA assay. Figure 5E showed that both LPS and MWCNTs significantly increased the binding indicating activation of NF-κB to form a functional DNA-binding complex. Taken together, these results revealed that MWCNTs activated the canonical NF-κB signaling pathway to control the transcription of inflammatory cytokines and chemokines in macrophages.

Induction of TGFβ1, PDGF, and Fibroblast-to-Myofibroblast Transformation. In addition to damaging lung cells and stimulating macrophages to secrete inflammatory mediators, fibrogenic agents induce fibrotic reactions characterized by increased production of profibrogenic growth factors, such as TGFβ1 and PDGF, proliferation and differentiation of fibroblasts into myofibroblasts, and secretion of type 1 collagen by myofibroblasts. We examined whether MWCNTs induce these fibrotic phenotypes in lung cells. We found that the mRNA and protein levels of TGFβ1 and PDGF in BEAS-2B and WI38-VA13 cells (Figure 6) as well as macrophages (data not shown) treated with MWCNTs at 20 μg/mL for 24 h were significantly increased, similarly to treatment with LPS or IL-1β, known inducers of TGFβ1 and PDGF.

We examined whether MWCNTs induce the transformation of fibroblast to myofibroblast. It is believed that TGFβ1 and PDGF secreted from macrophages and lung epithelial cells serve as critical paracrine stimuli to fibroblasts to promote the transformation of fibroblasts into myofibroblasts. Myofibroblasts synthesize the characteristic αSMA to enhance their contractile force and secretes collagen I to deposit in the matrix resulting in fibrosis. We analyzed the expression of αSMA in lung fibroblast cells. We first treated macrophages with MWCNT (20 μg/mL, 16 h) or LPS (1 μg/mL, 5 h, as positive control). The culture medium was collected and centrifuged to remove residual cells and MWCNTs; the supernatant was designated as "MWCNT-conditioned medium". WI38VA-13 fibroblasts were then cultured in the MWCNT-conditioned medium for 24 h. Expression of αSMA was measured by using fluorescent microscopy with specific antibodies against αSMA. As shown in Figure 7, a significant increase in the fluorescence intensity of αSMA was observed in fibroblasts cultured in the MWCNT-conditioned medium. The results indicated that MWCNT stimulated macrophages to secret soluble factors, such as TGFβ1 and PDGF, which in turn function as paracrines to promote differentiation of the fibroblasts into myofibroblasts.

■ DISCUSSION

Exposure to fibrogenic materials and chemicals causes pulmonary injury that typically progresses into lung interstitial fibrosis, granulomatous fibrosis, or mesothelioma.[1,2,35] Studies

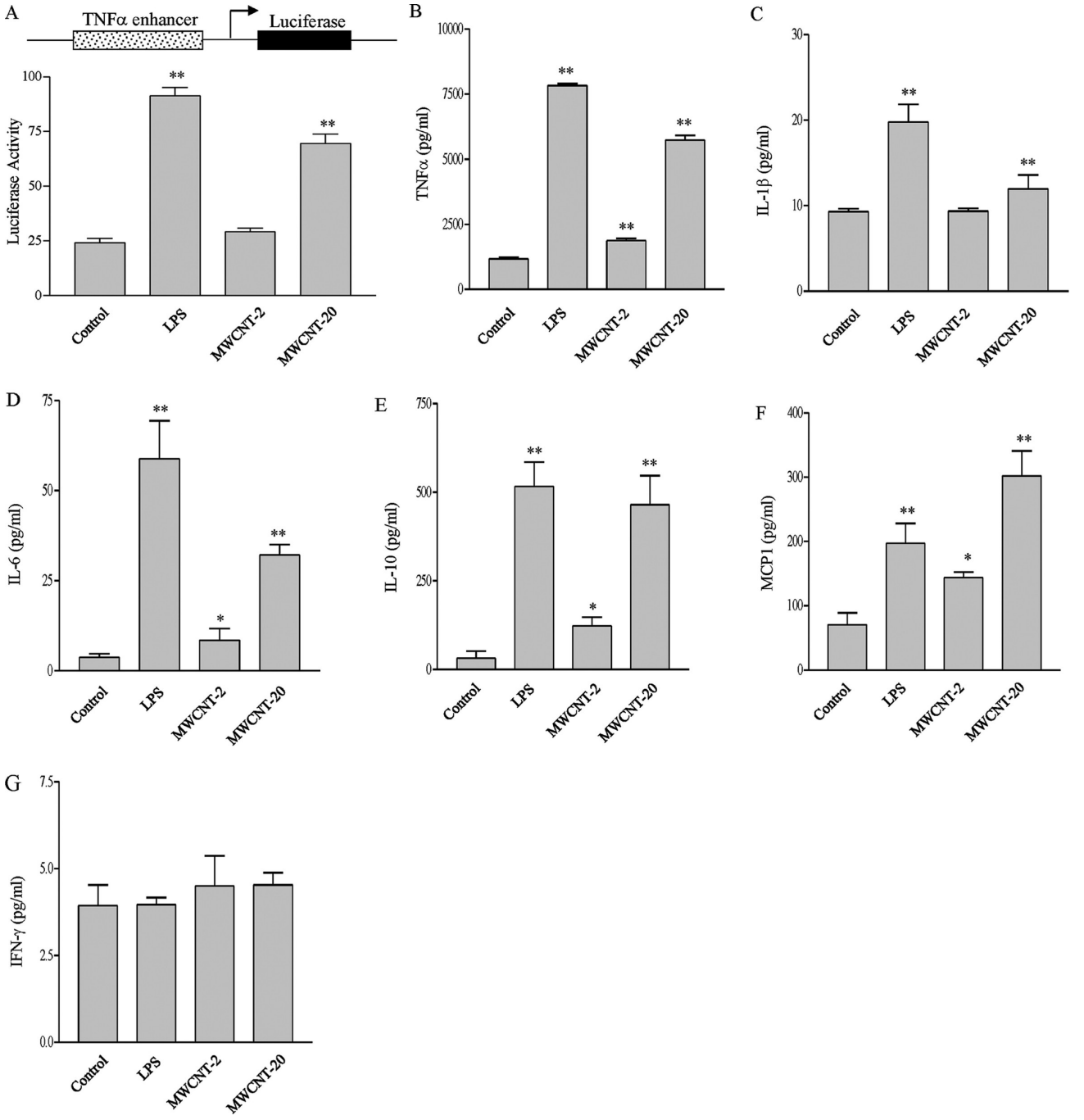

Figure 4. Induction of cytokines and chemokines. (A) TNFα luciferase reporter expression. RAW264.7 cells stably transfected with the TNFα promoter/luciferase reporter construct were treated with MWCNTs at 0, 2, and 20 μg/mL for 16 h. LPS at 1 μg/mL for 5 h was used as a positive control. Luciferase activity was measured. (B–G) Endogenous cytokine and chemokine expression. RAW264.7 cells were treated as for panel A. Cell-free culture medium was collected, and cytokines and chemokines were detected by flow cytometry using mouse cytometric bead array and Flex beads. Data represent means ± SDs from three samples. *, $p < 0.05$, and **, $p < 0.01$, as compared with control.

of the underlying mechanisms for fibrotic lesions revealed that injury to the airway and alveolar epithelial cells, activation of macrophages, and fibroblast-to-myofibroblast transformations are common cellular events during lung fibrosis,[6,7] whereas the molecular steps mediating the events remain unclear.

CNTs are newly discovered forms of crystalline carbon that form cylinders of carbon with nanometer diameters and varying lengths. Animal studies indicated that CNTs damage the lungs, penetrate through lung tissues, and induce fibrotic lesions in lung interstitium and pleura.[13,14,17−23] The cellular and molecular mechanisms by which CNTs induce lung toxicity and fibrosis are unclear. We addressed this issue by examining the interactions between MWCNTs and lung cells at molecular levels. Our results are consistent with previous studies that MWCNTs are pulmonary fibrogenic inducers.[19,22] These findings suggest a molecular and cellular framework for MWCNT lung toxicity, in which MWCNTs stimulate oxidative stress and mitochondrial damage to cause injuries to lung epithelial cells, activate NF-κB signaling to boost inflammatory and profibrogenic cytokine and growth factor production and

dx.doi.org/10.1021/tx200351d | Chem. Res. Toxicol. 2011, 24, 2237−2248

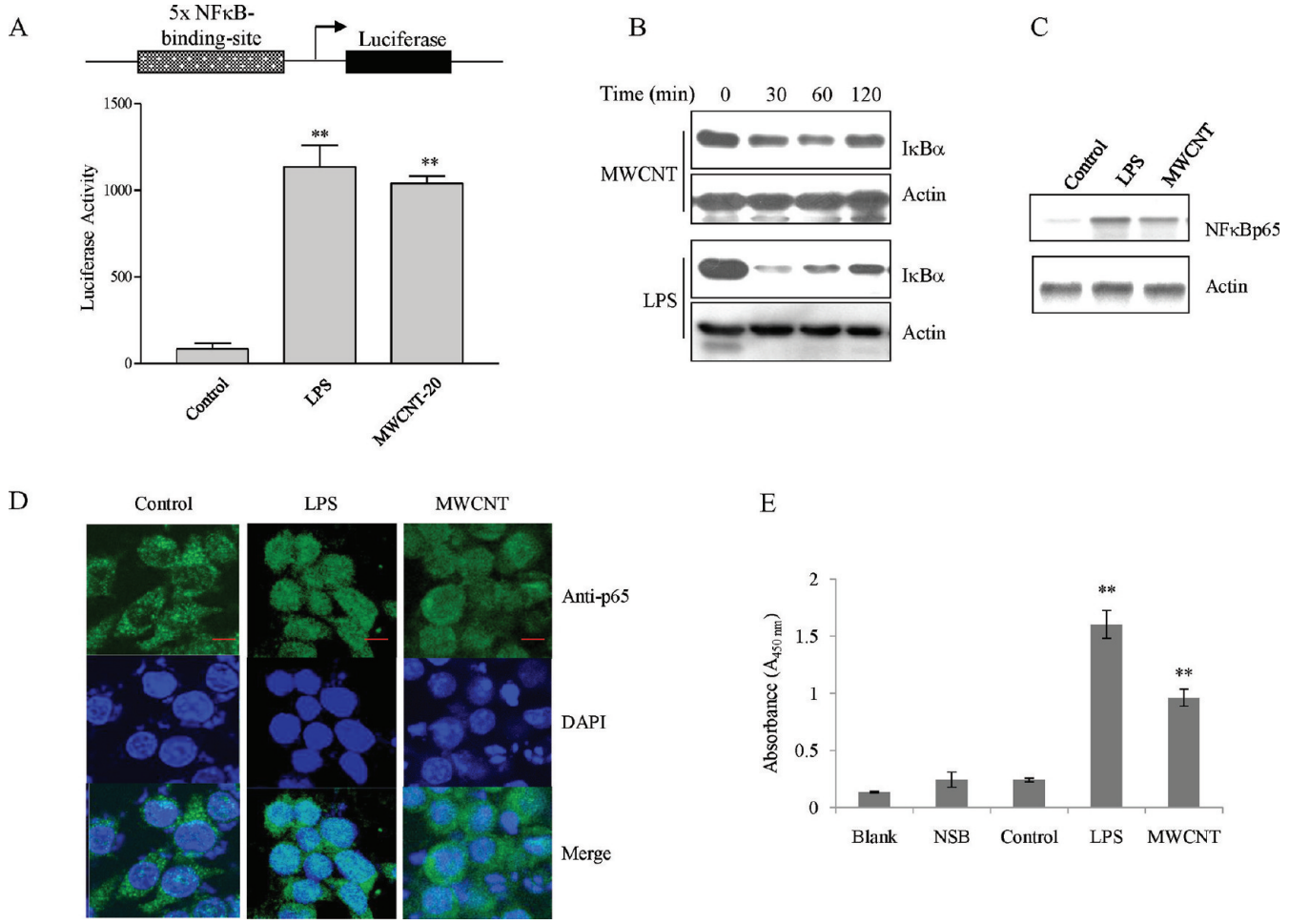

Figure 5. Activation of NF-κB signaling. (A) NF-κB binding site/luciferase reporter expression. RAW264.7 cells were stably transfected with a luciferase reporter gene expression construct under the control of five copies of the synthetic NF-κB binding site. The cells were treated with MWCNTs or LPS as described for Figure 4. Luciferase activity was measured. (B) IκB degradation. Macrophages were treated with MWCNTs at 20 μg/mL for 0, 30, 60, and 120 min. LPS (1 μg/mL) was used as a positive control. The cell lysate was immunoblotted against IκBα. Actin was used as a loading control. (C) Immunoblotting of nuclear NF-κB. Nuclear extracts from cells treated with LPS (1 μg/mL, 5 h) or MWCNT (20 μg/mL, 16 h) were immunoblotted with anti-NF-κBp65. Actin was used as a loading control. (D) Fluorescent microscopy of nuclear NF-κB. Cells cultured in eight-well chamber slides were treated with LPS (positive control) at 1 μg/mL for 5 h or MWCNT at 20 μg/mL for 16 h. Cells were stained with anti-NF-κBp65 antibodies, followed by Alexia 488-conjugated secondary antibody. Images were taken under a confocal fluorescent microscope; bar size = 10 μm. (E) Binding of NF-κB to DNA. Cells were treated with LPS (1 μg/mL) for 5 h or MWCNTs (20 μg/mL) for 16 h. Binding of NF-κB to NF-κB-binding element was measured using nuclear extracts and the NF-κB p65 ELISA assay kit. NSB, nonspecific binding. Data represent means ± SDs from three samples. **, $p < 0.01$.

secretion, and promote the fibroblast-to-myofibroblast transformation for the synthesis of collagen and αSMA that are important for matrix deposition and remodeling, ultimately resulting in lung fibrosis. Given that many other fibrogenic agents including fibers and particles (silica, asbestos, and coal dust particles),[5,36] anticancer drugs (bleomycin),[37] metals (chromium), and pesticides (paraquat)[4] also induce oxidative stress, inflammation, and proliferation of fibroblasts, we propose that our molecular model of MWCNT lung toxicity is applicable to fibrosis by these agents.

ROS are produced as a byproduct of cellular respiration in the mitochondria or to serve a physiological function, such as killing microbes by phagocytes during infection and stimulating cell growth.[5] ROS also result from exposure to toxicants. In the case of fibrogenic fibers, ROS can be formed via radicals on the surface or surface-bound chemicals such as quinines that can undergo redox cycling to generate superoxide anions and hydrogen peroxide. Alternatively, fibers can damage the mitochondria to increase ROS production. Excessive ROS results in oxidative stress that promotes cell death and activates specific signaling pathways, both implicated in the pathogenesis of lung fibrosis.[5] We found that MWCNTs induced significant ROS production in bronchial and alveolar epithelial cells and fibroblasts. ROS production correlated with MWCNT-induced cell toxicity and was observed at subtoxic doses. Parallel to ROS production, MWCNTs induced substantial depolarization of mitochondrial inner membrane potential, indicating mitochondrial damage. Similar results were found by others in NR8383 and A549 cells.[38,39] Using a cell-free system, Finoglio et al. showed that MWCNT increased ROS production but did not directly generate free radicals.[40] Long, straight CNTs stimulated IL-1β production from macrophages through a ROS-mediated process because the antioxidant trolox effectively diminished CNT-induced IL-1β secretion.[41] Together, these findings suggest that mitochondrial damage is likely a common mechanism by which CNTs induce oxidative stress

dx.doi.org/10.1021/tx200351d | Chem. Res. Toxicol. 2011, 24, 2237–2248

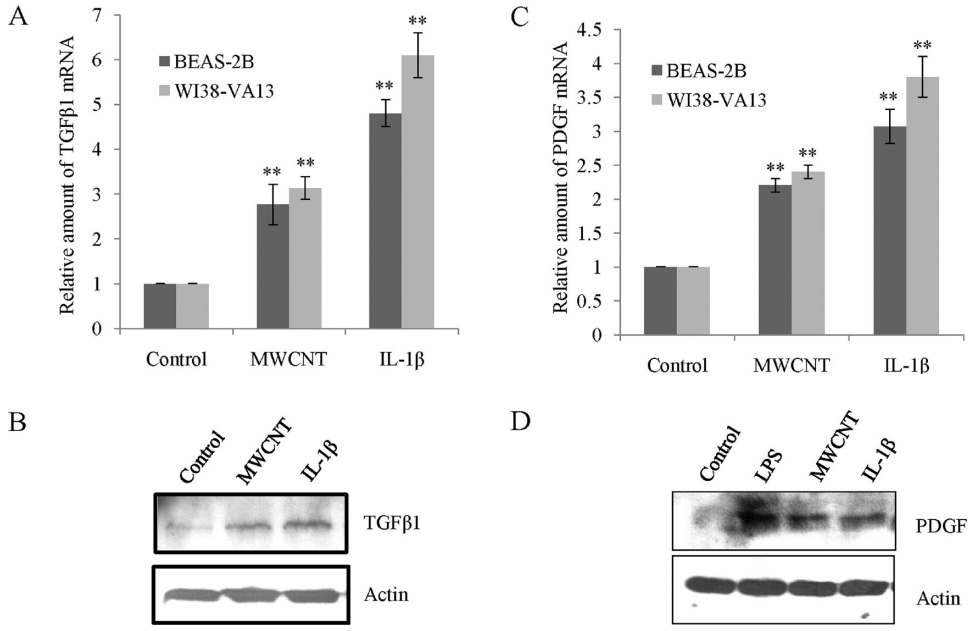

Figure 6. Induction of TGFβ1 and PDGF. BEAS-2B and WI38-VA13 cells were treated with MWCNTs (20 μg/mL, 24 h), LPS (1 μg/mL, 5 h), or IL-1β (5 ng/mL, 24 h), respectively. (A) Real-time PCR for TGFβ1 mRNA. (B) Immunoblotting of TGFβ1 protein. (C) Real-time PCR for PDGF mRNA. (D) Immunoblotting of PDGF protein. GAPDH was used as a loading control. In C and D, results from BEAS-2B cells are shown. **, $p < 0.01$, as compared with control.

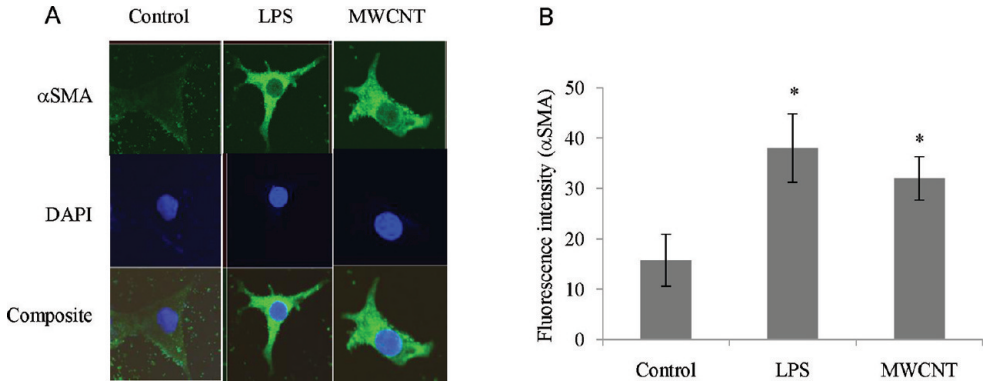

Figure 7. Induction of αSMA. (A) Myofibroblast transformation. Macrophages were treated with MWCNTs (20 μg/mL, 16 h) or LPS (1 μg/mL, 5 h). The culture medium free of cells and MWCNTs was collected as MWCNT-conditioned medium. WI38-VA13 fibroblasts were then cultured in the MWCNT-conditioned medium in eight-well chamber slides for 24 h. Expression of αSMA was detected by immunofluorescent staining of the cells with an anti-αSMA antibody followed by an alexia-488 conjugated secondary antibody. The nucleus was stained with DAPI. Cell images were taken under a Zeiss LSM510 confocal microscope. (B) Quantitative data of panel A from five separate fields. *, $p < 0.05$, as compared with control.

and cause toxicity to lung cells. This finding raises the possibility of employing antioxidants or other agents that suppress ROS production and oxidative damage for the prevention and treatment of CNT lung toxicity and fibrosis.

MWCNTs induce pulmonary inflammation in mice dose dependently. In one study, exposure to MWCNT at doses approximating the estimated human occupational exposure induced pulmonary inflammation and damage peaking at 7 days postexposure. Pulmonary fibrosis was observed by 7 days and granulomatous inflammation persisted throughout 56 days.[22] MWCNT was also found to penetrate lung tissues to reach the pleura.[22] In a separate study, inflammatory cytokines were induced in mice treated with subcutaneous injection of MWCNT.[42] We showed here that MWCNT induced a panel of inflammatory cytokines and chemokines including TNFα, IL-1β, IL-6, IL-10, and MCP1, which are commonly elevated during lung inflammation and fibrosis. Furthermore, we demonstrated that induction of the inflammatory mediators by MWCNT is mediated through the canonical pathway of NF-κB signaling, in which MWCNT induced the ubiquitination and proteasomal degradation of IκBα, increased the nuclear accumulation of NF-κBp65 protein, enhanced the binding of NF-κB to NF-κB-binding sequences in DNA, and transactivated TNFα promoter for transcription. Our study was the first to systematically analyze the pathway through which MWCNT activate NF-κB and induce inflammatory cytokines and chemokines. In addition to regulating cytokine expression, NF-κB modulates TGFβ signaling in collagen synthesis and PDGF transcription to impact fibrosis.[29−31]

How MWCNTs activate the canonical pathway is unclear. LPS is known to activate NF-κB via the canonical pathway by binding to its receptor TLR4 on the plasma membrane.[25] Activated TLR4 recruits adapter molecules including MyD88 and Tirap within the cytoplasm of cells to propagate a signal to

activate IKKs and the NF-κB pathway. Presumably, signaling molecules that are produced upon exposure to MWCNTs, such as ROS, interact with molecules in the pathway to activate NF-κB. Alternatively, MWCNTs may stimulate the activation of RAGE (receptor for advanced glycation endproduct) to activate NF-κB. RAGE is known to be activated and is responsible for the activation of NF-κB under a range of oxidative and disease conditions, such as Alzheimer's disease and familial amyloidotic polyneuropathy.[43,44] Further studies are needed to investigate these possibilities.

Persistent cellular damage and inflammation in the lungs lead to fibrosis and other chronic pathologies such as cancer. Although the carcinogenic potential of CNTs remains to be defined, MWCNTs appear to potently induce lung interstitial fibrosis and mesothelioma in a number of rodent models.[13,17,19−22] A key cellular mediator of fibrosis is myofibroblast.[6,7] Myofibroblasts are the primary collagen-producing cells and are responsible for the de novo synthesis of characteristic αSMA. Collagen is the major fiber-forming component in the matrix for fibrosis, whereas αSMA incorporates into stress fibers to increase contractile force. Contraction by myofibroblasts is transmitted to the extracellular matrix by means of focal adhesion structures (i.e., fibronexus) for cell migration and scar formation. Pulmonary mesenchymal cells (mainly fibroblasts) that give rise to myofibroblasts can derive directly from resident lung mesenchymal cells, by recruiting circulating fibrocytes, or through epithelial-mesenchymal transition. Transformation of fibroblasts into myofibroblasts is controlled via several complex mechanisms, including paracrine signals from macrophages and lung epithelial cells and autocrine functions of fibroblasts and myofibroblasts. Among the paracrines, PDGF stimulates the proliferation and migration of fibroblasts, whereas TGFβ1 promotes the fibroblast-to-myofibroblat transformation and subsequent matrix synthesis by myofibroblasts. We found that MWCNTs stimulate the expression and secretion of both PDGF and TGFβ1 from macrophages, lung bronchial epithelial cells, and fibroblasts. Furthermore, we demonstrated, for the first time, that MWCNT-induced growth factors served as paracrine signals to stimulate the differentiation of fibroblasts into myofibroblasts as evidenced by the de novo synthesis of αSMA in the cells. These findings put constraints on the possible mechanisms by which MWCNT induce fibrosis in the lungs at cellular and molecular levels.

CNTs differ considerably in structure, size, shape, surface charge and chemistry, agglomeration, metal content, and purity, which may influence their deposition and toxicity in the lungs.[12,38,45] We have used a commercially available, well-characterized MWCNT in the study. Our findings were consistent with studies using MWCNTs from different sources in different systems.[19,22] The functionalization of CNTs changes their surface chemistry and potentially their interactions with biological systems. For instance, the functionalization of CNTs with carboxyl groups on the surface would increase the solubility and interaction of CNT with cell membrane raising the potentials of CNTs for drug delivery and diagnostics.[46] Experimental data indicated that acid treatment of CNTs reduces their potential for cytotoxicity and inflammation, which is, in part, attributable to reduced metal contents after acid wash.[46,47] On the other hand, increased solubility would enhance the dispersion and distribution of CNTs in the lungs, which would, ultimately, increase fibrosis.[48] The MWCNT used in the study was treated with diluted hydrochloric acid to remove the catalyst Co−MgO during manufacture that potentially introduced carboxyl groups on the surface of the MWCNT. The infrared vibrational spectrum of pristine CNT is typically nearly featureless, whereas carbonyl groups from the carboxylation of CNTs would display a very strong, narrow feature near 1700 cm^{-1}. The spectrum of the MWCNT revealed by FTIR was nearly featureless with no apparent absorption features near 1700 cm^{-1}. Therefore, we conclude that there are very few, if any, carbonyl groups on the MWCNT.

While our study is focused on the mechanistic analysis of the molecular actions of MWCNTs in lung cells, this molecular toxicity pathway-based in vitro study avoids using a large amount of animals and provides a simple and quick molecular toxicity assessment method that can be adopted for high-throughput screening of CNTs and other nanomaterials in vitro. Such an approach would facilitate a direct comparison among different CNTs and other nanoparticles for lung toxicity and fibrosis. Identification of structural, physical, and chemical properties of CNT that cause toxicity and fibrosis through these rapid toxicity screening would help engineer safer and more effective CNT products.[49] Finally, our mechanistic study suggests potential, novel targets that can be exploited for the development of therapeutic and preventive measures against lung fibrosis by CNTs and other fibrogenic toxicants for future studies.

AUTHOR INFORMATION

Corresponding Author

*Tel: 304-285-6241. Fax: 304-285-5708. E-mail: qam1@cdc.gov.

ABBREVIATIONS

CNT, carbon nanotubes; DHE, dihydroethium; FTIR, Fourier transform infrared spectroscopy; HRTEM, high-resolution transmission electron microscopy; IL, interleukin; INF, interferon; LPS, lipopolysaccharide; MCP1, monocyte chemotactic protein-1; MTDR, Mitotrack deep red 633; MWCNT, multiwalled carbon nanotube; PDGF, platelet-derived growth factor; ROS, reactive oxygen species; αSMA, α-smooth muscle actin; SWCNT, single-walled carbon nanotube; TEM, transmission electron microscopy; TGF, transforming growth factor; TMRE, tetramethylrodamine ester; TNF, tumor necrosis factor.

REFERENCES

(1) Rom, W. N. (2007) Asbestosis, pleural fibrosis, and lung cancer. In *Envriornmental and Occupational Medicine* (Rom, W. N., and Markowitz, S. B., Eds.) pp 298−316, Lippincott Williams & Wilkins, Philadelphia.

(2) Castranova, V., and Vallyathan, V. (2000) Silicosis and coal workers' pneumoconiosis. *Environ. Health Perspect. 108* (Suppl.4), 675−684.

(3) Cho, H. Y., Reddy, S. P., Yamamoto, M., and Kleeberger, S. R. (2004) The transcription factor NRF2 protects against pulmonary fibrosis. *FASEB J. 18*, 1258−1260.

(4) Bus, J. S., and Gibson, J. E. (1984) Paraquat: Model for oxidant-initiated toxicity. *Environ. Health Perspect. 55*, 37−46.

(5) Ma, Q. (2010) Transcriptional responses to oxidative stress: Pathological and toxicological implications. *Pharmacol. Ther. 125*, 376−393.

(6) Bonner, J. C. (2010) Mesenchymal cell survival in airway and interstitial pulmonary fibrosis. *Fibrogenesis Tissue Repair 3*, 15.

(7) Wynn, T. A. (2008) Cellular and molecular mechanisms of fibrosis. *J. Pathol. 214*, 199−210.

(8) Fichtner-Feigl, S., Strober, W., Kawakami, K., Puri, R. K., and Kitani, A. (2006) IL-13 signaling through the IL-13alpha2 receptor is involved in induction of TGF-beta1 production and fibrosis. *Nat. Med. 12*, 99−106.
(9) Harris, P. J. F. (2009) *Carbon Nanotube Science*, Cambridge University Press, Cambridge.
(10) Maynard, A. D., Baron, P. A., Foley, M., Shvedova, A. A., Kisin, E. R., and Castranova, V. (2004) Exposure to carbon nanotube material: Aerosol release during the handling of unrefined single-walled carbon nanotube material. *J. Toxicol. Environ. Health, Part A 67*, 87−107.
(11) Maynard, A. M., and Kuempel, E. D. (2005) Airborne nanostructured particles and occupational health. *J. Nanopart. Res. 7*, 587−614.
(12) Donaldson, K., Aitken, R., Tran, L., Stone, V., Duffin, R., Forrest, G., and Alexander, A. (2006) Carbon nanotubes: A review of their properties in relation to pulmonary toxicology and workplace safety. *Toxicol. Sci. 92*, 5−22.
(13) Ryman-Rasmussen, J. P., Cesta, M. F., Brody, A. R., Shipley-Phillips, J. K., Everitt, J. I., Tewksbury, E. W., Moss, O. R., Wong, B. A., Dodd, D. E., Andersen, M. E., and Bonner, J. C. (2009) Inhaled carbon nanotubes reach the subpleural tissue in mice. *Nat. Nanotechnol. 4*, 747−751.
(14) Choi, H. S., Ashitate, Y., Lee, J. H., Kim, S. H., Matsui, A., Insin, N., Bawendi, M. G., Semmler-Behnke, M., Frangioni, J. V., and Tsuda, A. (2010) Rapid translocation of nanoparticles from the lung airspaces to the body. *Nat. Biotechnol. 28*, 1300−1303.
(15) Lam, C. W., James, J. T., McCluskey, R., Arepalli, S., and Hunter, R. L. (2006) A review of carbon nanotube toxicity and assessment of potential occupational and environmental health risks. *Crit. Rev. Toxicol. 36*, 189−217.
(16) Balbus, J. M., Maynard, A. D., Colvin, V. L., Castranova, V., Daston, G. P., Denison, R. A., Dreher, K. L., Goering, P. L., Goldberg, A. M., Kulinowski, K. M., Monteiro-Riviere, N. A., Oberdorster, G., Omenn, G. S., Pinkerton, K. E., Ramos, K. S., Rest, K. M., Sass, J. B., Silbergeld, E. K., and Wong, B. A. (2007) Meeting report: hazard assessment for nanoparticles—Report from an interdisciplinary workshop. *Environ. Health Perspect. 115*, 1654−1659.
(17) NTRC, N. (2009) *Approaches to Safe Nanotechnology. Managing the Health and Safety Concerns Associated with Engineered Nanomaterials*, www.cdc.gov/niosh/docs/2009-125/, National Insititute for Occupational Safety and Health, (DHHS) Publication 2009-125, Cincinnati.
(18) Porter, A. E., Gass, M., Muller, K., Skepper, J. N., Midgley, P. A., and Welland, M. (2007) Direct imaging of single-walled carbon nanotubes in cells. *Nat. Nanotechnol. 2*, 713−717.
(19) Mercer, R. R., Hubbs, A. F., Scabilloni, J. F., Wang, L., Battelli, L. A., Schwegler-Berry, D., Castranova, V., and Porter, D. W. (2010) Distribution and persistence of pleural penetrations by multi-walled carbon nanotubes. *Part. Fibre Toxicol. 7*, 28.
(20) Poland, C. A., Duffin, R., Kinloch, I., Maynard, A., Wallace, W. A., Seaton, A., Stone, V., Brown, S., Macnee, W., and Donaldson, K. (2008) Carbon nanotubes introduced into the abdominal cavity of mice show asbestos-like pathogenicity in a pilot study. *Nat. Nanotechnol. 3*, 423−428.
(21) Takagi, A., Hirose, A., Nishimura, T., Fukumori, N., Ogata, A., Ohashi, N., Kitajima, S., and Kanno, J. (2008) Induction of mesothelioma in p53± mouse by intraperitoneal application of multi-wall carbon nanotube. *J. Toxicol. Sci. 33*, 105−116.
(22) Porter, D. W., Hubbs, A. F., Mercer, R. R., Wu, N., Wolfarth, M. G., Sriram, K., Leonard, S., Battelli, L., Schwegler-Berry, D., Friend, S., Andrew, M., Chen, B. T., Tsuruoka, S., Endo, M., and Castranova, V. (2010) Mouse pulmonary dose- and time course-responses induced by exposure to multi-walled carbon nanotubes. *Toxicology 269*, 136−147.
(23) Shvedova, A. A., Kisin, E. R., Mercer, R., Murray, A. R., Johnson, V. J., Potapovich, A. I., Tyurina, Y. Y., Gorelik, O., Arepalli, S., Schwegler-Berry, D., Hubbs, A. F., Antonini, J., Evans, D. E., Ku, B. K., Ramsey, D., Maynard, A., Kagan, V. E., Castranova, V., and Baron, P. (2005) Unusual inflammatory and fibrogenic pulmonary responses to single-walled carbon nanotubes in mice. *Am. J. Physiol. Lung Cell Mol. Physiol. 289*, L698−708.
(24) Hubbs, A. F., Mercer, R. R., Benkovic, S. A., Harkema, J., Sriram, K., Schwegler-Berry, D., Goravanahally, M. P., Nurkiewicz, T. R., Castranova, V., and Sargent, L. M. (2010) Nanotoxicology—A pathologist's perspective. *Toxicol. Pathol. 39*, 301−324.
(25) Gilmore, T. D. (2006) Introduction to NF-kappaB: Players, pathways, perspectives. *Oncogene 25*, 6680−6684.
(26) Agostini, C., and Gurrieri, C. (2006) Chemokine/cytokine cocktail in idiopathic pulmonary fibrosis. *Proc. Am. Thorac. Soc. 3*, 357−363.
(27) Gabbiani, G. (2003) The myofibroblast in wound healing and fibrocontractive diseases. *J. Pathol. 200*, 500−503.
(28) Anscher, M. S., Peters, W. P., Reisenbichler, H., Petros, W. P., and Jirtle, R. L. (1993) Transforming growth factor beta as a predictor of liver and lung fibrosis after autologous bone marrow transplantation for advanced breast cancer. *N. Engl. J. Med. 328*, 1592−1598.
(29) Kon, A., Vindevoghel, L., Kouba, D. J., Fujimura, Y., Uitto, J., and Mauviel, A. (1999) Cooperation between SMAD and NF-kappaB in growth factor regulated type VII collagen gene expression. *Oncogene 18*, 1837−1844.
(30) Khachigian, L. M., Resnick, N., Gimbrone, M. A. Jr., and Collins, T. (1995) Nuclear factor-kappa B interacts functionally with the platelet-derived growth factor B-chain shear-stress response element in vascular endothelial cells exposed to fluid shear stress. *J. Clin. Invest. 96*, 1169−1175.
(31) Au, P. Y., Martin, N., Chau, H., Moemeni, B., Chia, M., Liu, F. F., Minden, M., and Yeh, W. C. (2005) The oncogene PDGF-B provides a key switch from cell death to survival induced by TNF. *Oncogene 24*, 3196−3205.
(32) Wang, Y., Iqbal, Z., and Mitra, S. (2006) Rapidly functionalized, water-dispersed carbon nanotubes at high concentration. *J. Am. Chem. Soc. 128*, 95−99.
(33) Ma, Q., Kinneer, K., Ye, J., and Chen, B. J. (2003) Inhibition of nuclear factor kappaB by phenolic antioxidants: Interplay between antioxidant signaling and inflammatory cytokine expression. *Mol. Pharmacol. 64*, 211−219.
(34) He, X., Kan, H., Cai, L., and Ma, Q. (2009) Nrf2 is critical in defense against high glucose-induced oxidative damage in cardiomyocytes. *J. Mol. Cell. Cardiol. 46*, 47−58.
(35) Husain, A. N., and Kuman, V. (2005) The Lung. In *Robbins and Cotran Pathologic Basis of Disease* (Kumar, V., Abbas, A. K., and Fausto, N., Eds.) pp 711−772, Elsevier Saunders, Philadelphia.
(36) Castranova, V. (2004) Signaling pathways controlling the production of inflammatory mediators in response to crystalline silica exposure: role of reactive oxygen/nitrogen species. *Free Radical Biol. Med. 37*, 916−925.
(37) Cho, H. Y., Reddy, S. P., and Kleeberger, S. R. (2006) Nrf2 defends the lung from oxidative stress. *Antioxid. Redox Signaling 8*, 76−87.
(38) Pulskamp, K., Diabate, S., and Krug, H. F. (2007) Carbon nanotubes show no sign of acute toxicity but induce intracellular reactive oxygen species in dependence on contaminants. *Toxicol. Lett. 168*, 58−74.
(39) Manna, S. K., Sarkar, S., Barr, J., Wise, K., Barrera, E. V., Jejelowo, O., Rice-Ficht, A. C., and Ramesh, G. T. (2005) Single-walled carbon nanotube induces oxidative stress and activates nuclear transcription factor-kappaB in human keratinocytes. *Nano Lett. 5*, 1676−1684.
(40) Fenoglio, I., Tomatis, M., Lison, D., Muller, J., Fonseca, A., Nagy, J. B., and Fubini, B. (2006) Reactivity of carbon nanotubes: free radical generation or scavenging activity? *Free Radical Biol. Med. 40*, 1227−1233.
(41) Brown, D. M., Donaldson, K., and Stone, V. (2010) Nuclear translocation of Nrf2 and expression of antioxidant defence genes in THP-1 cells exposed to carbon nanotubes. *J. Biomed. Nanotechnol. 6*, 224−233.
(42) Meng, J., Wang, D. L., Wang, P. C., Jia, L., Chen, C., and Liang, X. J. (2010) Biomedical activities of endohedral metallofullerene

optimized for nanopharmaceutics. *J. Nanosci. Nanotechnol. 10*, 8610−8616.
(43) Sousa, M. M., Yan, S. D., Stern, D., and Saraiva, M. J. (2000) Interaction of the receptor for advanced glycation end products (RAGE) with transthyretin triggers nuclear transcription factor kB (NF-kB) activation. *Lab. Invest. 80*, 1101−1110.
(44) Forbes, J. M., Soderlund, J., Yap, F. Y., Knip, M., Andrikopoulos, S., Ilonen, J., Simell, O., Veijola, R., Sourris, K. C., Coughlan, M. T., Forsblom, C., Slattery, R., Grey, S. T., Wessman, M., Yamamoto, H., Bierhaus, A., Cooper, M. E., and Groop, P. H. (2011) Receptor for advanced glycation end-products (RAGE) provides a link between genetic susceptibility and environmental factors in type 1 diabetes. *Diabetologia 54*, 1032−1042.
(45) Lanone, S., Rogerieux, F., Geys, J., Dupont, A., Maillot-Marechal, E., Boczkowski, J., Lacroix, G., and Hoet, P. (2009) Comparative toxicity of 24 manufactured nanoparticles in human alveolar epithelial and macrophage cell lines. *Part. Fibre Toxicol. 6*, 14.
(46) Sayes, C. M., Liang, F., Hudson, J. L., Mendez, J., Guo, W., Beach, J. M., Moore, V. C., Doyle, C. D., West, J. L., Billups, W. E., Ausman, K. D., and Colvin, V. L. (2006) Functionalization density dependence of single-walled carbon nanotubes cytotoxicity in vitro. *Toxicol. Lett. 161*, 135−142.
(47) Kagan, V. E., Tyurina, Y. Y., Tyurin, V. A., Konduru, N. V., Potapovich, A. I., Osipov, A. N., Kisin, E. R., Schwegler-Berry, D., Mercer, R., Castranova, V., and Shvedova, A. A. (2006) Direct and indirect effects of single walled carbon nanotubes on RAW 264.7 macrophages: Role of iron. *Toxicol. Lett. 165*, 88−100.
(48) Mercer, R. R., Scabilloni, J., Wang, L., Kisin, E., Murray, A. R., Schwegler-Berry, D., Shvedova, A. A., and Castranova, V. (2008) Alteration of deposition pattern and pulmonary response as a result of improved dispersion of aspirated single-walled carbon nanotubes in a mouse model. *Am. J. Physiol. Lung Cell Mol. Physiol. 294*, L87−L97.
(49) George, S., Pokhrel, S., Xia, T., Gilbert, B., Ji, Z., Schowalter, M., Rosenauer, A., Damoiseaux, R., Bradley, K. A., Madler, L., and Nel, A. E. (2010) Use of a rapid cytotoxicity screening approach to engineer a safer zinc oxide nanoparticle through iron doping. *ACS Nano 4*, 15−29.